Towards high efficiency thin-film crystalline silicon solar cells: The roles of light trapping and non-radiative recombinations

A. Bozzola,[a] P. Kowalczewski, and L. C. Andreani
Physics Department, University of Pavia and CNISM, via Bassi 6, I-27100 Pavia, Italy

Thin-film solar cells based on silicon have emerged as an alternative to standard thick wafers technology, but they are less efficient, because of incomplete absorption of sunlight, and non-radiative recombinations. In this paper, we focus on the case of crystalline silicon (c-Si) devices, and we present a full analytic electro-optical model for p-n junction solar cells with Lambertian light trapping. This model is validated against numerical solutions of the drift-diffusion equations. We use this model to investigate the interplay between light trapping, and bulk and surface recombination. Special attention is paid to surface recombination processes, which become more important in thinner devices. These effects are further amplified due to the textures required for light trapping, which lead to increased surface area. We show that c-Si solar cells with thickness of a few microns can overcome 20% efficiency and outperform bulk ones when light trapping is implemented. The optimal device thickness in presence of light trapping, bulk and surface recombination, is quantified to be in the range of 10–80 μm, depending on the bulk quality. These results hold, provided the effective surface recombination is kept below a critical level of the order of 100 cm/s. We discuss the possibility of meeting this requirement, in the context of state-of-the-art techniques for light trapping and surface passivation. We show that our predictions are within the capability of present day silicon technologies. © 2014 AIP Publishing LLC. [http://dx.doi.org/10.1063/1.4867008]

I. INTRODUCTION

A central focus of crystalline silicon (c-Si) solar cell research is to conceive and realize novel structures that can be competitive with conventional wafer-based technologies, in terms of energy conversion efficiency *and* device costs. Thin-film solar cells have advantages in terms of material usage, but their efficiency is lower than that of bulk cells. Recent trends, in particular the loss of market share of many thin-film technologies such as those based on amorphous and micro-crystalline (μc-Si) silicon to more efficient bulk c-Si cells, show that high efficiency is becoming the most important evaluation criterion for photovoltaic (PV) technology. Therefore, research on novel structures should analyze the basic motivations for low efficiency in thin-film solar cells in more depth, and focus on those categories of devices that show a real margin of efficiency improvement, compared to standard wafer-based c-Si solar cells. The aim of this paper is to face this problem from a theoretical point of view, focusing on the basic physics of solar energy conversion in c-Si solar cells, with light trapping in realistic conditions, where non-radiative recombinations must be taken into account.

The first reason for low efficiency in thin-film devices is the incomplete absorption of light. While a remarkable 25% efficiency can be achieved in lab cells using high quality 400 μm thick pyramidal textured silicon wafers,[1,2] this value drops below 20% for thickness around 40 microns,[3] and even smaller values, when using thinner layers.[4–10] For this reason, increasing absorption by means of light trapping is advantageous.[11–27]

Conversion efficiency is also a matter of transport losses. These can be divided into two categories: *intrinsic*, including radiative and Auger recombinations, and *extrinsic* or Shockley-Read-Hall (SRH) recombination, induced by defects in the bulk and / or at the silicon interfaces.[28,29] While the former losses have been widely investigated for c-Si,[30–33] far less is known about *realistic* efficiency limits when the efficiency is dominated by extrinsic losses, which is the most common regime. Tiedje *et al.*[31] calculated the limits imposed by radiative and Auger recombination in c-Si solar cells with light trapping. These processes limit the ultimate efficiency to 29.8%, with an optimal silicon thickness of around 80 μm. These efficiency values are higher than in state-of-the-art devices (both bulk and thin-films), indicating that extrinsic losses are the dominant losses in real solar cells.

At the end of the 1990 s, Green incorporated surface recombination and Lambertian light trapping in a single electro-optical model.[34] However, this model does not employ the surface recombination velocity, but rather the open-circuit voltage. This quantity is dependent on the device structure, limiting extension of the model's applicability to other semiconductor materials and cell architectures.

It would be of great interest to determine the efficiency limits, and the optimal thickness, in a more general framework for solar cells incorporating light trapping and *extrinsic* recombinations, and to quantify the constraints on bulk and surface quality that allow these limits to be approached. Recent developments in the fabrication of thin *crystalline* silicon layers for solar cells, and especially those based on epitaxial growth,[3,35] liquid phase recrystalization,[36] and

[a]Electronic mail: angelo.bozzola@unipv.it; URL: http://fisica.unipv.it/nanophotonics/

annealing and reorganization of porous silicon wafers,[10,37] have given further motivation for this analysis.

In this work, we develop an analytic electro-optical model, which is validated against numerical solutions of drift-diffusion equations, to study p-n junctions c-Si solar cells with thickness between 500 nm and 200 μm. We assume Lambertian light randomization[38–41] as a means to increase absorption in the c-Si, and as the prototype for devices incorporating light trapping. Carrier transport inside the device is modelled within a general p-n junction framework, which is largely adopted in real c-Si devices. A crucial concern for efficiency is the role of surface recombination, which becomes important for thinner cells,[34] and which is increased by the micro- and nanostructuring required for light trapping, because of the increased surface area.[42,43] We find that surface recombination, at present technological level, does not affect the conclusion that silicon solar cells can be made at the same time *thinner* and *more efficient* than with conventional wafer technology. The novelty of this work lies in the analytic model; in the systematic investigation of the effects of non-radiative recombinations, and in a precise quantification of the surface recombination velocity allowing thin-film c-Si solar cells to outperform bulk ones.

The rest of the paper is organized as follows. In Sec. II, we present the analytic model, with a special focus on Lambertian light randomization and calculation of the carrier generation rate (Sec. II A), on the solution of drift-diffusion equations under sunlight (Sec. II B), and in the dark (Sec. II C). In Sec. III, we focus on the effects of light trapping and recombination in the bulk of the cell, which determine the optimal thickness. In Sec. IV, we explore how surface recombination in the presence of increased surface area affects the energy conversion efficiency and the optimal cell thickness. A challenging target of 20% efficiency is assumed. In Sec. V, we discuss the design requirements in terms of light trapping, bulk and surface qualities that allow the target to be reached. Details on the analytic solution of drift-diffusion equation are given in the Appendix.

II. THE ANALYTIC ELECTRO-OPTICAL MODEL

The crystalline silicon solar cell structures under investigation are sketched in Fig. 1. For planar cells (Fig. 1(a)), we choose a n$^+$-p junction design, with a semi-infinite silver back reflector and 80 nm thick transparent anti-reflection layer ($n = 2$, $k = 0$). Optical data for c-Si and Ag are taken from Palik, Ref. 44. Silver is chosen because of its higher reflectivity compared to other metals that are compatible with silicon technology (such as aluminium). The selected thickness and refractive index of the anti-reflection (AR) coating are chosen to be close to those of silicon nitride coatings, which are widely applied in c-Si solar cells. Although our framework allows calculating parasitic absorption in the multilayer, we prefer to focus on the electrical losses, and to avoid the transparent conducting oxide (TCO) absorption by assuming $k = 0$ (Fig. 1(a)). The n$^+$ region is 50 nm thick, with a donor concentration of 10^{19} cm^{-3}, while the rest of the cell is lightly p-doped, with an acceptor concentration of 10^{16} cm^{-3}. The selected doping levels are representative of p-n junction c-Si
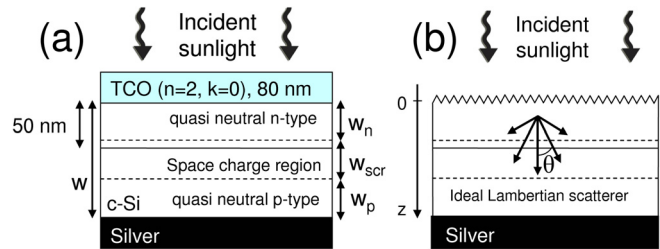

FIG. 1. The structures under investigation: planar solar cell (a) and solar cell with Lambertian light-trapping (b).

solar cells[28] and make SRH recombination the dominant mechanism in the device.[45] As a consequence of doping, a space charge region (SCR) develops across the junction plane. We adopt the framework of depletion region approximation.[28] The SCR of width w_{scr} is totally depleted of free carriers, and two quasi-neutral (qn) regions of widths w_n and w_p set up in the n- and p-type silicon, as shown in Fig. 1. These widths are calculated solving the Poisson equation across the junction plane.[28] With the selected values for dopants concentrations, we obtain $w_{scr} = 350$ nm, and the SCR is almost totally localized to the lightly doped p-side of the device. Consequently, increasing the cell thickness leads to a thicker qn region in the p-type material.

For the case of light trapping (Fig. 1(b)), we assume the same doping levels and no reflection losses at the front surface. Lambertian light randomization is defined in such a way that all incident light is transmitted to the active medium (no reflection losses), and the intensity scattered at an angle θ from the surface normal (Fig. 1(b)) is proportional to $\cos\theta$.[38–41] Each angular component is characterized by its optical path, which is enhanced according to $1/\cos\theta$ with respect to the planar case. If θ is larger than the critical angle $\arcsin(1/n_{Si})$, light is trapped inside the silicon slab by total internal reflection. As for the case of flat cells, a silver back reflector is assumed at the bottom. In Sec. II A, a brief comparison between silver and ideal back reflector (unit reflectance) will be presented for solar cells with Lambertian light trapping.

The choice of limiting to the case of zero reflection losses is dictated by two reasons: (i) defining an upper limit to active absorption, and (ii) dealing with state-of-the-art texturing for light trapping, which do reduce reflection losses to a large extent. The case of finite reflection losses at the front surface can be treated following Ref. 39. Part of the incident light may be back-scattered, and the resulting carrier generation rate and photocurrent will be lower than in our case. Several authors already reported very low reflection around 1%–2%, or even less, in the visible and near-infrared (NIR) ranges, in silicon wafers[1,2] and epi-layers.[3] In these cases, the front surface of the silicon cell is textured, and then coated with AR coating materials, such as silicon nitride or silicon dioxide. Reaching the Lambertian limit with zero reflection losses thus seems within the technological capability, at least when using a silicon thickness larger than a few tens of microns.

Other solutions for light trapping that are capable of approaching the Lambertian limit in thin-films have been proposed, e.g., in the theoretical Refs. 23–27. In all cases,

the Lambertian limit can be reached, and even overcome, at specific wavelengths. The most demanding part is to achieve this level of absorption for all wavelengths that are relevant for solar cell operation. Up to now, no working device based on thin-film c-Si showed absorption and photocurrent close to those of the Lambertian limit treated in this paper. In this sense, this field of research still needs some time before reaching the same maturity level of c-Si wafers.

It is worth remarking that front surface textures for light trapping increase the surface area compared to a flat, unpatterned device such as that depicted in Fig. 1(a). As it will be described in the next paragraphs, this surface area enhancement is a crucial factor for electrical transport in presence of surface recombination, and it is has to be carefully taken into account.

Our electro-optical model consists of three steps: (A) the calculation of the carrier generation rate, (B) the solution of diffusion equations for photogenerated minority carriers, and (C) the calculation of the total current density $J(V)$ under applied bias V. Of course, in order to get analytic solutions some approximations are needed. The impact of these approximations will be traced, when presenting the results and relative numerical validations. Generally speaking, these approximations can be divided into two categories: those needed to reduce the 3D electro-optical problem to a simpler 1D problem, and those strictly related to transport modelling. The first approximations are essential in order to obtain a model that depends only on the variable z (Fig. 1), and allow calculating analytic solutions. The second category allows for a simpler description of the transport process within the p-n junction; the most important of which is the depletion region approximation.[28]

A. Calculation of the carrier generation rates

We calculate the carrier generation rate $g(z, E)$ in planar cells using Poynting vector analysis.[46] Assuming normally incident sunlight along the z direction (Fig. 1), and a Poynting vector amplitude of S_0, the carrier generation rate is

$$g(z, E) = -\left[\frac{1}{S_0}\frac{dS_z}{dz}\right]\phi_{AM1.5}(E). \quad (1)$$

We use a transfer matrix approach to calculate the forward and backward electric field amplitudes E_{Si}^+ and E_{Si}^- at the beginning of the silicon slab ($z = 0$).[46] This leads to an analytic expression for S_z, and for the carrier generation rate in flat cells of

$$g(z, E) = 2n_{Si}k_{Si}k_0[|E_{Si}^+|^2 e^{-2k_{Si}k_0 z} + |E_{Si}^-|^2 e^{2k_{Si}k_0 z}$$
$$+ 2\Im(E_{Si}^+ E_{Si}^{-*})\sin(2n_{Si}k_0 z)$$
$$- 2\Re(E_{Si}^+ E_{Si}^{-*})\cos(2n_{Si}k_0 z)]\phi_{AM1.5}(E), \quad (2)$$

where n_{Si} (k_{Si}) denotes the real (imaginary) parts of the refractive index of silicon, k_0 is the incident wave vector, and $\phi_{AM1.5}$ is the incident AM 1.5 photon flux. The exponential terms in Eq. (2) represent the attenuation of the forward and backward propagating waves, while the sine and cosine terms describe the effects of interference.[46]
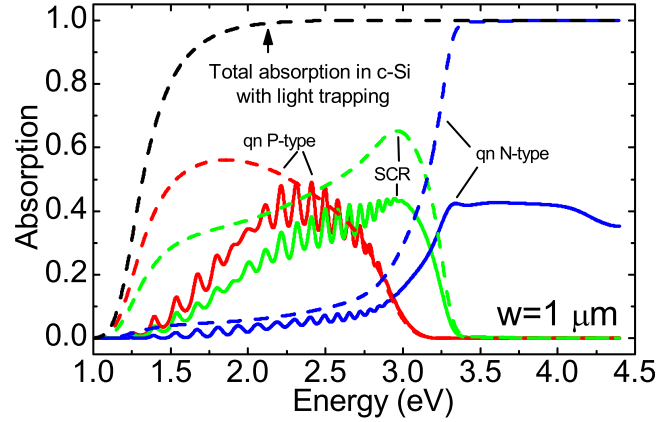

FIG. 2. Effects of light-trapping on the absorption within the SCR and qn regions. Solid lines refer to the planar case, while dash lines refer to light-trapping. Total absorption with light-trapping is also reported (see arrow). The silicon thickness w is set to 1 μm.

For the case of Lambertian light trapping, the Poynting vector in the structure is the sum of two contributions; (i) a hemispherical, downward propagating power flux, and (ii) the other corresponding case for upward propagation.[39] As a consequence, interference terms do not appear in the carrier generation rate. After averaging over the two polarization states and over all propagation directions inside the silicon, g may be written as

$$g(z, E) = \frac{\alpha_{lt}(R_b e^{-2\alpha_{lt}w} e^{\alpha_{lt}z} + e^{-\alpha_{lt}z})}{1 - R_b e^{-2\alpha_{lt}w}\left(1 - \frac{1}{n_{Si}^2}\right)}\phi_{AM1.5}. \quad (3)$$

Here, R_b is the silicon/silver interface reflectance, averaged over all polarizations and incidence directions, and α_{lt} is the effective absorption coefficient of c-Si, in presence of Lambertian light trapping. α_{lt} is proportional to the intrinsic absorption coefficient of c-Si, α, through $\alpha_{lt} = \alpha(w_{eff}/w)$, where the term in brackets represents the effective light path enhancement as calculated by Green.[39]

The effects on absorption within the SCR and qn regions of 1 μm thick solar cells are shown in Fig. 2. Light path enhancement, and the suppression of reflection losses, strongly increase the sunlight absorption in c-Si, which is close to that of thick wafers with just a few microns of active material.

Equation (3) is fundamental to reduce the full 3D optical problem of solar cells with real textures to a simpler and versatile 1D prototype. It is worth noticing that although it is simple and subject to approximations,[38,39] Eq. (3) provides a reasonable estimation of *where* light is absorbed within the film. This is shown in Fig. 3, where we report the ratio $g(z, E)/\phi_{AM1.5}(E)$ for solar cells with silicon thicknesses of 10, 25, and 50 μm, at $E = 1.5$ eV. These structures either incorporate an optimized front layer with Gaussian roughness[20] (solid lines) and are modelled exactly using Rigorous Coupled Wave Analysis (RCWA),[47] or include Lambertian light trapping (dashed lines), using Eq. (3). The two decay profiles are very similar in the bulk of the active material, after the rough region. Notice that the lack of interference follows from light trapping, which randomizes the propagation directions.[39] This is expressed by Eq. (3) and confirmed by RCWA results.
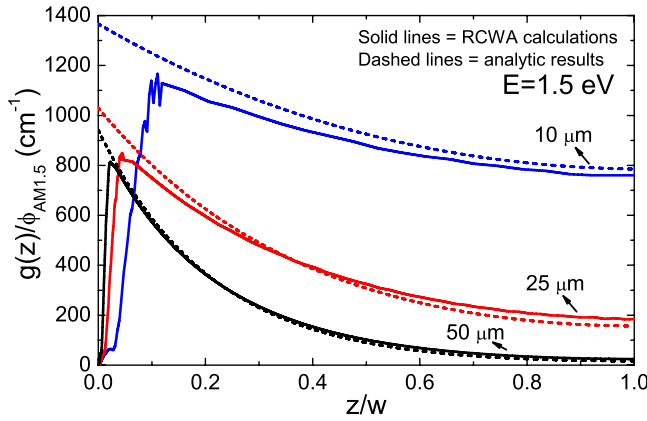
FIG. 3. Carrier generation rate normalized to AM 1.5 photon flux for c-Si solar cells incorporating an optimized front layer with Gaussian roughness,[20] calculated using RCWA (solid lines), and for cells with the Lambertian light trapping and the same silicon thickness (dashed lines), calculated using Eq. (1).

B. Dynamics of photogenerated carriers

The next step of modelling is the analytic solution of the diffusion equations for the excess minority carriers.[28,48,49] For electrons in the p region, which represent the major contribution to photocurrent, we have

$$D_p \frac{d^2 \Delta n}{dz^2} - \frac{\Delta n}{\tau_p} + g(z,E) = 0, \tag{4}$$

where D_p is the diffusion constant, and τ_p is the electron lifetime in p-type material, which is linked to diffusion length via $L_p = \sqrt{D_p \tau_p}$. The surface recombination velocity enters into the boundary conditions,[28,48,49] as specified below. It is worth noticing that for cells with light trapping, the surface area may be increased by micro-structuring. This causes a larger surface recombination current, with respect to a flat design of the same surface quality (i.e., same concentration of defects per unit area). In the following, we take this fact into account by introducing the effective surface recombination velocity

$$S_{\text{eff}} = K_{\text{area}} S = \frac{A_{\text{text}}}{A_{\text{flat}}} S, \tag{5}$$

where the K_{area} term represents the proposed geometrical surface area increase.[42]

The boundary conditions for Eq. (4) may be written as

$$\Delta n(z = w_n + w_{scr}) = 0, \tag{6}$$

$$\left. \frac{d\Delta n}{dz} \right|_{z=w} = -\frac{S_{\text{eff,p}}}{D_p} \Delta n(z = w). \tag{7}$$

Equations (5) and (7) are important in reducing the transport problem of textured solar cells from a 3D problem to a 1D problem, so that an analytic solution can be found. This is illustrated in the Appendix. An analogous treatment holds for holes in the heavily doped n-type qn region of the cell.

Once analytic solutions for Δn are found, the contribution to external quantum efficiency (EQE) from the p-type qn region is analytically obtained as $\text{EQE}_p(E) = \frac{D_p}{\phi_{AM1.5}} \frac{d\Delta n}{dz} \Big|_{z=w_n+w_{scr}}$. A similar treatment holds for excess holes in qn n-type material.

We assume that carriers generated within the SCR are collected with a quantum efficiency of unity, thanks to the sweeping action of the built-in electric field.[28,48,49] The EQE contribution from the SCR is obtained by integrating the (normalized) carrier generation rates of Eqs. (2) and (3) over the width of the SCR

$$EQE_{scr}(E) = \int_{z=w_n}^{z=w_n+w_{scr}} \frac{g(z,E)}{\phi_{AM1.5}(E)} dz. \tag{8}$$

C. J(V) curve of the devices

The solar cells $J(V)$ curves are calculated as superposition between photogenerated and dark diode currents, approximating the former term with the short-circuit current: $J(V) = J_{sc} - J_{\text{dark}}(V)$. The short-circuit current is calculated from the EQE spectrum as $J_{sc} = \int EQE(E)\phi_{AM1.5}(E)dE$.

The dark current density J_{dark} is expressed as the sum of three contributions from the qn regions and SCR, as for the case of the J_{sc}.[28] Dark JV terms from qn regions are proportional to $\exp(eV/k_B T)$ and include the effects of thickness and SRH recombinations, both in the bulk and at the surfaces. Usually, the dark current from the p-type silicon is the dominant term, as this qn region is typically the thicker one in the device. The contribution from the SCR has a different bias dependence, and it is proportional to $\sinh(eV/2k_B T)/(V_{bi} - V)$, where V_{bi} is the built-in voltage determined by the selected dopings, which is equal to 0.89 V.[28]

Therefore, the energy conversion efficiency η depends on the main electrical parameters: $\eta = FF \times J_{sc} V_{oc} / P_{inc}$, where FF is the fill factor, V_{oc} the open-circuit voltage, and $P_{inc} = 100$ mW/cm^2 (AM 1.5 spectrum). When calculating J_{dark} we neglect the shrinkage of the SCR induced by applied bias V. In this way, the dark JV is always slightly underestimated; and consequently, V_{oc} and η are slightly overestimated. Using our model, we can now focus on the energy conversion efficiency, which is the natural figure of merit for photovoltaic devices.

III. EFFECTS OF SILICON THICKNESS AND BULK SRH RECOMBINATION

As the first step of our analysis, we investigate the role of the cell thickness for both (i) planar and (ii) light trapping based devices; these two results are shown in Fig. 4, using triangular and circular symbols, respectively. At this point, we assume an ideal surface passivation ($S_n = S_p = 0$ cm/s), and a bulk material quality that is representative of c-Si at the PV module level, namely $D_p = 40$ cm^2/s, $D_n = 2$ cm^2/s, $L_p = 200\,\mu$m, and $L_n = 20\,\mu$m.[28] Light trapping boosts the active absorption, improving the short-circuit current. The impact of light trapping on the V_{oc} is rather small because this depends logarithmically on the J_{sc}.[28] We see that the thickness drastically affects all cell parameters. As shown by the curves with triangles, thin planar cells suffer from poor absorption, which limits J_{sc} well below the maximum value of 43 mA/cm^2 (Fig. 4(a)). On the other hand, V_{oc} has the opposite behaviour (Fig. 4(d)). These trends determine a maximum in conversion efficiency. As shown in Fig. 4(b), for planar
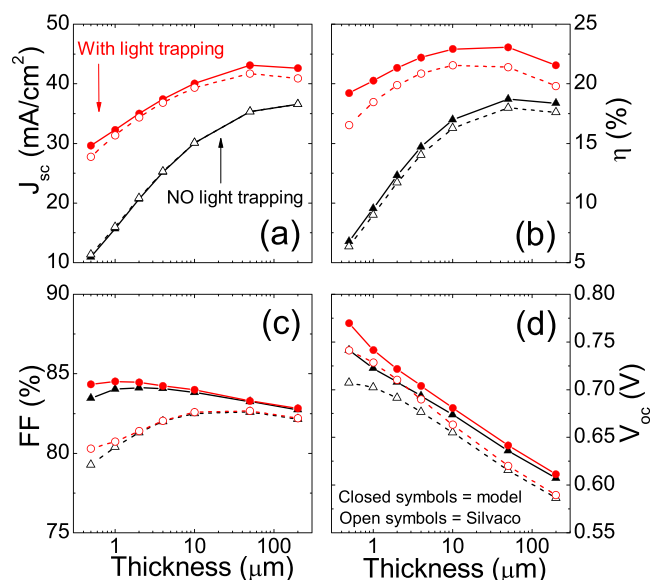
FIG. 4. The main electric parameters for c-Si solar cells with perfect surface passivation ($S_n = S_p = 0$ cm/s): short-circuit current density J_{sc} (a), conversion efficiency η (b), fill factor FF (c), and open-circuit voltage V_{oc} (d). Analytic results are reported with closed symbols (triangles for the planar case, and circles for the light-trapping case) and connecting lines, while numerical results from Silvaco ATLAS are reported with open symbols and dashed connecting lines.

cells, the maximum is in the range 50–100 μm; and for the case of light trapping, the optimal thickness reduces to 30 μm.

We validate our results against finite-elements solutions of drift-diffusion equation obtained with the Silvaco ATLAS device simulator: results are reported in Fig. 4 with dashed lines and open symbols. For these calculations, we assumed the same cell architecture and recombination parameters, but the carriers dynamics are calculated from the numerical solution of the transport equations. The Lambertian carrier generation rate of Eq. (3) is used as the input for the ATLAS calculations. The aim of this validation is to check the impact of the approximations used to arrive at analytic results. As shown in Fig. 4, the agreement is satisfactory for J_{sc}, proving that the assumption of ideal collection from the SCR does not lead to a substantial overestimation of photogenerated current. V_{oc} and efficiency are systematically overestimated in the analytic model (by less than 10%). This is mainly due to the superposition approximation used in the calculation of the JV curve. In fact, the approximation overestimates the photogenerated current, and underestimates the dark current, at the same time. This affects all the cell's calculated electrical parameters. However, we see that the discrepancy in efficiency is nearly independent of the cell thickness, and that the general trend is well reproduced. A full validation of the model, in presence of surface recombination, is presented in Sec. IV.

We calculated the quantities of Fig. 4 for the same structures with an ideal back reflector with reflectance of unity (not shown). We verified that silver is rather close to the ideal case. J_{sc} decreases by no more than 2 mA/cm^2, while the absolute decrease of conversion efficiency is of the order of 1% compared to the case of the ideal metal. The impact on V_{oc}, FF, and optimal thickness is substantially negligible.
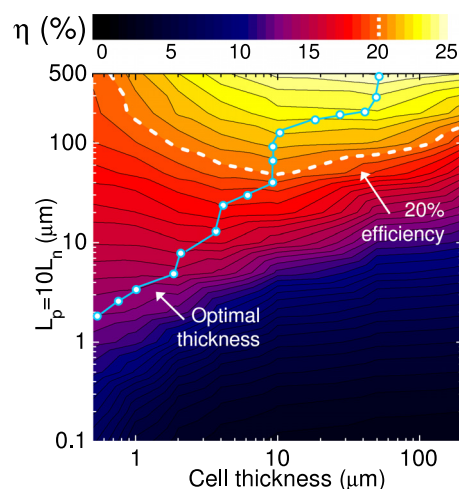

FIG. 5. Energy conversion efficiency for solar cells with Lambertian light trapping and perfect surface passivation ($S_n = S_p = 0$ cm/s) as a function of the bulk quality ($L_p = 10L_n$) and cell thickness. The useful range with η exceeding 20% is reported within a white dashed line, while the optimal configurations lie along the blue solid line.

The bulk material quality affects the collection of photogenerated carriers and consequently the conversion efficiency. This is shown in the contour plot of Fig. 5, where we report the energy conversion efficiency of solar cells with Lambertian light trapping, perfect surface passivation, and different thickness and bulk material quality. Here, we assume $L_p = 10L_n$ as for the other calculations in this paper. To be competitive against standard wafer technology, thin-film solar cells with light trapping must have comparable conversion efficiency. We fix the target to a value of 20%, which is a challenge when working with thin materials and non-wafer based technologies. This value is indicated in Fig. 5 by a dashed white line.

As evident from the contour plot, very thin c-Si solar cells with thickness down to 1 μm can also reach 20% efficiency, provided they offer good light trapping and material quality. We see that, for a given bulk quality, the efficiency is maximized at a given optimal thickness. This trend for the optimal thickness is illustrated in Fig. 5 by a blue line and symbols (the spread of values is due to numerical variance, which is amplified by the fact that the efficiency remains close to maximum over a wide range of thickness). We note that the optimal thickness increases with the bulk quality, but is always below the intrinsic limit of 80 μm, even for high quality materials.

The results of Fig. 5 offer the possibility to compare crystalline and micro-crystalline silicon materials, which are characterized by similar dielectric functions and absorption coefficients.[52,53] At first approximation, these materials absorb the same amount of sunlight, but the bulk material quality of μc-Si is rather poor compared to that of high quality c-Si wafers, with L of the order of a few μm, instead of hundreds of μm.[52,53] With such a poor bulk quality, the optimal thickness is only a few microns. For higher bulk qualities, as it is typically achieved in c-Si, the optimal thickness increases to a few tens of microns. We note that diffusion lengths in the base have to be larger than at least 60–70 μm to achieve 20% efficiency. Only crystalline silicon can meet this

requirement. Micro-crystalline materials in a single junction configuration can barely achieve 10% efficiency,[1] even in the presence of broad-band light trapping, despite much progress having been made in the last years to improve efficiency.[5–9]

We remark that the results of Fig. 5 have a definite practical relevance. They allow the optimal silicon thickness to be estimated without performing multiple time consuming numerical calculations, and without the need of a working device for empirical measurements. In fact, the minority carriers diffusion lengths are routinely extracted using different time-resolved spectroscopic techniques, such as photoluminescence or photo conductance decay measurements. By varying the sample thickness[50] and / or the excitation wavelength,[51] the bulk parameters can be effectively separated from those of the surface, without the need of a finished working solar cell. Once the bulk quality is inferred, the optimal thickness of interest for device fabrication can be readily deduced from Fig. 5.

The results of this section clearly point to the thickness range of 10–80 μm being the most interesting one for high efficiency silicon solar cells with light trapping: in Sec. IV, we will see how surface dynamics impact this result.

IV. EFFECTS OF SURFACE RECOMBINATION IN TEXTURED DEVICES

For cells with Lambertian light trapping, the effects of surface recombination and increased surface area on the cell efficiency are illustrated in Fig. 6. We assume a standard material with bulk qualities of $L_n = 20\,\mu$m and $L_p = 200\,\mu$m, as in Fig. 4. For simplicity, we assume that the effective surface recombinations are the same; $S_{n,eff} = S_{p,eff}$. Of course, this may not be the general case in real solar cells, where top and bottom surfaces may be very different, and where only one of them may be patterned for the purpose of light trapping. However, this choice does not significantly affect our conclusions. Figure 6(a) is calculated using our model, while Fig. 6(b) is obtained with ATLAS calculations. Comparing the plots, we note that the analytic model overestimates the conversion efficiency (the relative error is less than 10%) as discussed in Fig. 4(b). However, we note that the trend as a function of S and thickness is well reproduced, giving a validation to the model, over the explored range of parameters. The JV curves for a c-Si thickness of 10 μm and different values of the effective surface recombination velocity S_{eff} is shown in Fig. 6(c). Curves obtained with the analytic model are reported with solid lines, while those obtained with the ATLAS software are reported with dashed lines. Equal S_{eff} are assumed at both surfaces. We see that also in presence of surface recombination, the model slightly overestimates the cell parameters, with the same behaviour described in Sec. III.

The plots in Figs. 6(a) and 6(b) show that there is an upper limit for S, below which the efficiency has a maximum, and thin cells with light trapping are more efficient than bulk ones. This value is around $S_{eff} = 10^3$ cm/s. Above this value, surface dynamics drastically impact the overall efficiency, making a bulk design the best choice.

When effective surface recombination velocities are below 10^2 cm/s, the ultimate efficiency is approached. In this
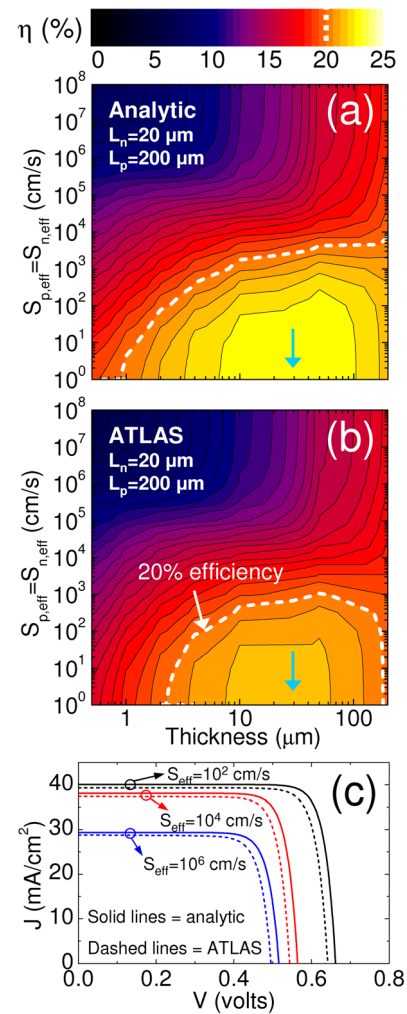

FIG. 6. Effects of solar cells thickness and effective surface recombination velocity on the conversion efficiency η for solar cells incorporating Lambertian light trapping: analytic (a) and ATLAS results (b). JV curves for c-Si solar cells with thickness 10 μm, and $S_{eff} = 10^2$ cm/s (black lines), $S_{eff} = 10^4$ cm/s (red lines), and $S_{eff} = 10^6$ cm/s (blue lines) (c). Analytic results are reported with solid lines, while ATLAS results with dashed lines. In all cases, Lambertian light trapping is assumed, and $L_n = 20\,\mu$m, $L_p = 200\,\mu$m.

case, the device can be considered as substantially free of surface losses, and efficiency is determined only by the bulk quality and light trapping, as for the case of Fig. 5. However, we note that the optimal thickness is around 30 μm, when S_{eff} is below 10^2 cm/s. This result goes beyond previous ones reported in Ref. 34, where it was shown that, as soon as surface recombination is introduced, the optimal thickness should move to the bulk regime (hundreds of μm or more). In fact, this happens only in the case of poorly passivated surfaces with $S_{eff} > 10^3$ cm/s; while for $S_{eff} < 10^2$ cm/s, the optimal thickness is always below the intrinsic limit of 80 μm, dictated by radiative and Auger recombinations. The results of Ref. 34 referred to a regime of relatively high surface recombination, while the focus of the present work is on the regime of low surface recombination, as discussed below.

In Figs. 7(a) and 7(b) (analytic), we address a low and a high quality material with $L_n = 5$ μm, $L_p = 50$ μm, and $L_n = 50$ μm, $L_p = 500$ μm, respectively. When the effective
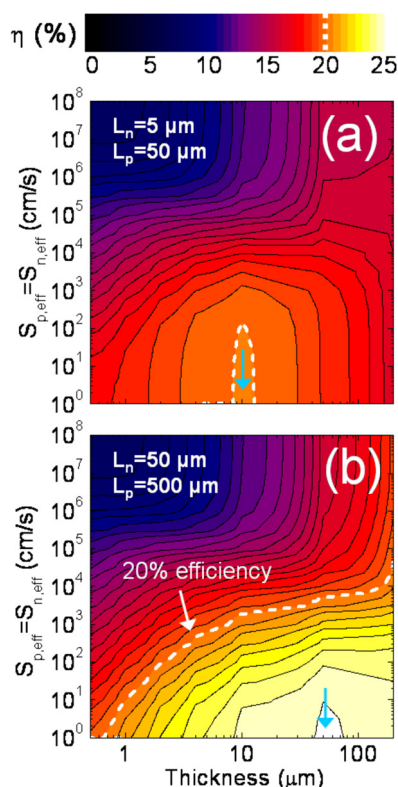
FIG. 7. Effects of solar cells thickness and effective surface recombination velocity on the conversion efficiency η for solar cells incorporating Lambertian light trapping: low quality silicon with $L_n = 5\,\mu m$, $L_p = 50\,\mu m$ (a), and high quality silicon with $L_n = 50\,\mu m$, $L_p = 500\,\mu m$ (b).

surface recombination velocity is below 10^3 cm/s, the ultimate efficiency and optimal thickness are determined only by the bulk quality and light trapping. In Fig. 6(a), the ultimate efficiency is 23.5%, with an optimal thickness around $30\,\mu m$. When the bulk material quality is worse (Fig. 7(a)), the ultimate efficiency drops to 20.1%, and the optimal thickness reduces to just $10\,\mu m$. The opposite trend occurs in high quality materials (Fig. 7(b)): the ultimate efficiency is around 25%, with an optimal thickness of $50\,\mu m$. Thus, we see that the optimal thickness is strongly correlated with the material quality and light trapping capability: this has yet to be taken into account for silicon device designs incorporating light trapping.

Finally, recalling that $S_{eff} = K_{area}\, S$, we see that the requirement in terms of surface passivation can also be achieved. It has already been shown that S can be reduced to a few cm/s or even less in silicon,[54,55] by applying thin passivating layers, and surface fields, by means of thin highly doped regions. S can also be reduced to comparable values (~ 10 cm/s) in nanostructured systems with complex morphology, by using conformal growth of the passivating layer, such as atomic layer deposition techniques.[56] To implement light trapping, surface nanostructuring has to be introduced and the effective surface area is increased accordingly. However, we note that any working photonic texture is characterized by typical features, which are comparable with the wavelengths of sunlight. In other words, there is no optical need for very complex morphologies with large K_{area} in order to scatter sunlight efficiently. We note

that an optimized 2D photonic lattice[19,43] yields an increased $K_{area} \sim 1.6$–1.7, while for a randomly rough surface with Gaussian disorder, such as that of Fig. 3, being very close to the Lambertian limit,[20] K_{area} is calculated as less than 2.5. We see that a S of the order of 10 cm/s, and a K_{area} of the order of 2.5, are largely compatible with the constraint for S_{eff} to be smaller than $\sim 10^2$ cm/s. Thus, the limiting values for the efficiency calculated here—when surface recombination is negligible, and solar cells in the range 10–80 μm outperform thicker ones—are well within the capabilities of current surface passivation technologies.

V. CONCLUSIONS

We have developed an analytic electro-optical model for p-n junction crystalline silicon solar cells, and we have used it to investigate the impact of light trapping and defects-mediated recombinations with a special focus on surface recombination and increased surface area. The results of this work give the overall requirements, in terms of bulk and surface qualities, to reach high efficiency in thin-film devices. We showed that a target value of 20% efficiency can be reached in a relatively wide range of cell thickness, and bulk and surface quality. The thickness range between 10 and $80\,\mu m$ seems to be the most interesting for high efficiency applications.

Three main ingredients are needed for thin devices to overcome the bulk cells

- Light trapping as close as possible to the Lambertian limit;
- Relatively high bulk quality (diffusion lengths of the order of a few hundreds of microns);
- Effective surface recombination below 10^2 cm/s.

We note that all these ingredients are achievable with present day technologies, although they have not yet been jointly implemented in a single device.

In fact, advanced photonic schemes allow for excellent trapping of sunlight not only in bulk c-Si wafers[2,28] but also in thin-films[22–27] down to the Wave Optics regime, where the device thickness is comparable with the typical wavelengths of sunlight. We note that, although the optical investigation of a few microns thick cells has attracted large attention in the last years, the calculated optimal thickness of c-Si devices with light trapping is larger, in the range 10–80 μm. This is the minimum thickness required to fully absorb most of the sunlight wavelengths, even with optimal Lambertian light trapping. Indeed, we note that such advanced light harvesting schemes are rather difficult to implement in real devices. In recent years, the investigation of light trapping structures started facing the problem of parasitic absorption in thin-film solar cells.[57–59] These are found to reduce light harvesting below the values of the Lambertian case investigated in this paper, although this is not expected to change the dependence on the cell thickness, as calculated in this work. In this sense, light trapping structures that allow absorbing sunlight only in the active parts of the devices will be crucial for further development of thin-film c-Si solar cells.

Very good control of the silicon thickness, and a bulk quality comparable or even superior to that of c-Si wafers for PV application, can be obtained using epitaxial layer deposition on a properly prepared silicon substrate. This technique is currently used to produce solar cells with thickness in the range 25–50 μm, with stabilized efficiency in the range 15%–19%,[1,3] and has a remarkable margin for improvement, with ultimate efficiencies exceeding those of thick wafers. Recent progresses in thin-film c-Si processing[37] open the way to future low cost substrates for high quality epitaxial growth.[35]

Finally, as recalled in Sec. V, surface losses can be drastically reduced by means of passivating layers, and a suitable electric design that incorporates surface fields. We believe that surface recombination velocities down to state-of-the-art values (a few cm/s or even less), and typical surface area enhancement K_{area} less than 2.5 could make c-Si solar cells with thickness 10-80 microns a real high efficiency alternative to wafer-based technology in the near future.

APPENDIX: ANALYTIC SOLUTION OF THE DIFFUSION EQUATION

The general solution of Eq. (4) for the case of flat solar cells can be split into two contributions: $\Delta n(z,E)_{exp}$ arising from exponential decay terms of Eq. (2), and $\Delta n(z,E)_{int}$ determined by the interference terms. The total electrons' concentration writes as

$$\Delta n(z,E) = \Delta n(z,E)_{exp} + \Delta n(z,E)_{int} = \frac{2n_{Si}k_{Si}k_0\phi_{AM1.5}L_p^2}{D_p(1-4k_{Si}^2k_0^2L_p^2)}\left[|E_{Si}^+|^2 e^{-2k_{Si}k_0z} + |E_{Si}^-|^2 e^{2k_{Si}k_0z}\right] + c_1 e^{z/L_p} + c_2 e^{-z/L_p}$$
$$+ \frac{4n_{Si}k_{Si}k_0\phi_{AM1.5}L_p^2}{D_p(1+4n_{Si}^2k_0^2L_p^2)}[\Re(E_{Si}^+E_{Si}^{-*})\cos(2n_{Si}k_0z) - \Im(E_{Si}^+E_{Si}^{-*})\sin(2n_{Si}k_0z)] + c_3 e^{z/L_p} + c_4 e^{-z/L_p}. \tag{A1}$$

The constants c_1, c_2, and c_3, c_4 are obtained inserting separately $\Delta n(z,E)_{exp}$ and $\Delta n(z,E)_{int}$ into the boundary conditions expressed by Eqs. (6) and (7) with $K_{area} = 1$. Denoting $h = w_n + w_{scr}$, the constants write as

$$c_1 = \frac{2n_{Si}k_{Si}k_0L_p^2\phi_{AM1.5}}{D_p(1-4k_{Si}^2k_0^2L_p^2)}\left\{|E_{Si}^+|^2\left[e^{-2k_{Si}k_0w}\left(2k_{Si}k_0 - \frac{S_p}{D_p}\right) - e^{-2k_{Si}k_0h-w_p/L_p}\left(\frac{1}{L_p} - \frac{S_p}{D_p}\right)\right]\right.$$
$$\left. + |E_{Si}^-|^2\left[e^{2k_{Si}k_0w}\left(-2k_{Si}k_0 - \frac{S_p}{D_p}\right) - e^{2k_{Si}k_0h-w_p/L_p}\left(\frac{1}{L_p} - \frac{S_p}{D_p}\right)\right]\right\}\bigg/\left[e^{w/L_p}\left(\frac{1}{L_p} + \frac{S_p}{D_p}\right) + e^{(2h-w)/L_p}\left(\frac{1}{L_p} - \frac{S_p}{D_p}\right)\right], \tag{A2}$$

$$c_2 = -c_1 e^{2h/L_p} - \frac{2n_{Si}k_{Si}k_0L_p^2\phi_{AM1.5}}{D_p(1-4k_{Si}^2k_0^2L_p^2)}[|E_{Si}^+|^2 e^{-2k_{Si}k_0h+h/L_p} + |E_{Si}^-|^2 e^{2k_{Si}k_0h+h/L_p}], \tag{A3}$$

$$c_3 = \frac{4n_{Si}k_{Si}k_0L_p^2\phi_{AM1.5}}{D_p(1+4n_{Si}^2k_0^2L_p^2)}\left\{R\left[2n_{Si}k_0\sin(2n_{Si}k_0w) - \frac{S_p}{D_p}\cos(2n_{Si}k_0w) - \cos(2n_{Si}k_0h)e^{-w_p/L_p}\left(\frac{1}{L_p} - \frac{S_p}{D_p}\right)\right]\right.$$
$$\left. + I\left[2n_{Si}k_0\cos(2n_{Si}k_0w) + \frac{S_p}{D_p}\sin(2n_{Si}k_0w) + \sin(2n_{Si}k_0h)e^{-w_p/L_p}\left(\frac{1}{L_p} - \frac{S_p}{D_p}\right)\right]\right\}$$
$$\bigg/\left[e^{w/L_p}\left(\frac{1}{L_p} + \frac{S_p}{D_p}\right) + e^{(2h-w)/L_p}\left(\frac{1}{L_p} - \frac{S_p}{D_p}\right)\right], \tag{A4}$$

$$c_4 = -c_3 e^{2h/L_p} - e^{h/L_p}\frac{4n_{Si}k_{Si}k_0L_p^2\phi_{AM1.5}}{D_p(1+4n_{Si}^2k_0^2L_p^2)}[R\cos(2n_{Si}k_0h) - I\sin(2n_{Si}k_0h)], \tag{A5}$$

where we denote $\Re(E_{Si}^+E_{Si}^{-*})$ as R, and $\Im(E_{Si}^+E_{Si}^{-*})$ as I.

For the case of solar cells with light trapping, the solution of Eq. (4) writes as

$$\Delta n(z,E) = \frac{\alpha_{lt}\left(R_b e^{-2\alpha_{lt}w}e^{\alpha_{lt}z} + e^{-\alpha_{lt}z}\right)}{D_p\left[1 - R_b e^{-2\alpha_{lt}w}(1 - 1/n_{Si}^2)\right]\left(1 - \alpha_{lt}^2 L_p^2\right)} + c_1 e^{z/L_p} + c_2 e^{-z/L_p}. \tag{A6}$$

The constants c_1 and c_2 are determined by the boundary conditions—Eqs. (6) and (7)—with $K_{\text{area}} > 1$

$$c_1 = \frac{\alpha_{lt}L_p^2\phi_{AM1.5}}{D_p(1 - R_b e^{-2\alpha_{lt}w}(1 - 1/n_{Si}^2))}\left[e^{-\alpha_{lt}w}\left(R_b\left(\alpha_{lt} + \frac{S_{eff,p}}{D_p}\right) - \alpha_{lt} + \frac{S_{eff,p}}{D_p}\right) + e^{-\alpha_{lt}h - w_p/L_p}(1 + R_b)\left(\frac{1}{L_p} - \frac{S_{eff,p}}{D_p}\right)\right]$$
$$\Bigg/ \left[e^{w/L_p}\left(\frac{1}{L_p} + \frac{S_{eff,p}}{D_p}\right) + e^{(2h-w)/L_p}\left(\frac{1}{L_p} - \frac{S_{eff,p}}{D_p}\right)\right], \tag{A7}$$

$$c_2 = -c_1 e^{2h/L_p} + \frac{\alpha_{lt}L_p^2\phi_{AM1.5}(1 + R_b)}{D_p(1 - R_b e^{-2\alpha_{lt}w}(1 - 1/n_{Si}^2))}e^{-\alpha_{lt}h + h/L_p}. \tag{A8}$$

An analogous treatment holds for holes in the n-type quasi neutral region.

[1]M. A. Green, K. Emery, Y. Hishikawa, W. Warta, and E. D. Dunlop, Prog. Photovoltaics **21**, 1–11 (2013).

[2]J. Zhao, A. Wang, M. A. Green, and F. Ferrazza, Appl. Phys. Lett. **73**(14), 1991–1993 (1998).

[3]J. H. Petermann, D. Zielke, J. Schmidt, F. Haase, E. G. Rojas, and R. Brendel, Prog. Photovoltaics **20**(1), 1–5 (2012).

[4]M. A. Green, P. A. Basore, N. Chang, D. Clugston, R. Egan, R. Evans, D. Hogg, S. Jamason, M. Keevers, P. Lasswell, J. O'Sullivan, U. Schubert, A. Turner, S. R. Wenham, and T. Young, Solar Energy **77**(6), 857–863 (2004).

[5]K. Söderström, G. Bugnon, F. J. Haug, S. Nicolay, and C. Ballif, Sol. Energy Mater. Sol. Cells **101**, 193–199 (2012).

[6]M. Meier, U. W. Paetzold, M. Prömpers, T. Merdzhanova, R. Carius, and A. Gordijn, "UV nanoimprint for the replication of etched ZnO:Al textures applied in thin-film silicon solar cells," Prog. Photovoltaics (published online).

[7]M. Boccard, C. Battaglia, S. Hänni, K. Söderström, J. Escarré, S. Nicolay, F. Meillaud, M. Despiesse, and C. Ballif, Nano Lett. **12**, 1344–1348 (2012).

[8]H. Sai, K. Saito, and M. Kondo, Appl. Phys. Lett. **101**, 173901 (2012).

[9]H. Sai, K. Saito, and M. Kondo, Appl. Phys. Lett. **102**, 053509 (2013).

[10]C. Trompoukis, O. El Daif, V. Depauw, I. Gordon, and J. Poortmans, Appl. Phys. Lett. **101**, 103901 (2012).

[11]P. Bermel, C. Luo, L. C. Kimerling, and J. D. Joannopoulos, Opt. Express **15**(25), 16986–17000 (2007).

[12]A. Bielawny, J. Upping, P. T. Miclea, R. B. Wehrspohn, C. Rockstuhl, F. Lederer, M. Peters, L. Steidi, R. Zentel, S. Lee, M. Knez, A. Lambertz, and R. Carius, Phys. Status Solidi A **205**(12), 2796–2810 (2008).

[13]O. Isabella, J. Krc, and M. Zeman, Appl. Phys. Lett. **97**, 101106 (2010).

[14]Z. Yu, A. Raman, and S. Fan, Proc. Natl. Acad. Sci. U.S.A. **107**(41), 17491–17496 (2010).

[15]T. Lanz, B. Ruhstaller, C. Battaglia, and C. Ballif, J. Appl. Phys. **110**, 033111 (2011).

[16]C. Battaglia, J. Escarré, K. Söderström, L. Erni, L. Ding, G. Bugnon, A. Billet, M. Boccard, L. Barraud, S. De Wolf, F. J. Haug, M. Despiesse, and C. Ballif, Nano Lett. **11**(2), 661–665 (2011).

[17]X. Meng, E. Drouard, G. Gomard, R. Peretti, A. Fave, and C. Seassal, Opt. Express **20**(S5), A560–A571 (2012).

[18]C. Battaglia, C. Hsu, K. Söderström, J. Escarré, F. J. Haug, M. Charrière, M. Boccard, M. Despiesse, D. T. L. Alexander, M. Cantoni, Y. Cui, and C. Ballif, ACS Nano **6**(3), 2790–2797 (2012).

[19]A. Bozzola, M. Liscidini, and L. C. Andreani, Opt. Express **20**(S2), A224–A244 (2012).

[20]P. Kowalczewski, M. Liscidini, and L. C. Andreani, Opt. Lett. **37**, 4868 (2012).

[21]E. R. Martins, J. Li, Y. K. Liu, J. Zhou, and T. F. Krauss, Phys. Rev. B **86**, 041404(R) (2012).

[22]O. Isabella, S. Solntsev, D. Caratelli, and M. Zeman, Prog. Photovoltaics **21**(1) 94–108 (2013).

[23]E. R. Martins, J. Li, Y. Liu, V. Depauw, Z. Chen, J. Zhou, and T. F. Krauss, Nat. Commun. **4**, 2665 (2013).

[24]K. X. Wang, Z. Yu, Y. Cui, and S. Fan, Nano Lett. **12**, 1616–1619 (2012).

[25]A. Bozzola, M. Liscidini, and L. C. Andreani, "Broadband light trapping with disordered photonic structures in thin-film silicon solar cells," Prog. Photovoltaics (published online).

[26]S. Eyderman, S. John, and A. Deinega, J. Appl. Phys. **113**, 154315 (2013).

[27]P. Kowalczewski, M. Liscidini, and L. C. Andreani, Opt. Express **21**(S5), A808–A820 (2013).

[28]J. Nelson, The Physics of Solar Cells (Imperial College Press, London, 2003).

[29]R. Brendel, Thin-Film Crystalline Silicon Solar Cells (Wiley-VCH, Weinheim, 2003).

[30]W. Shockley and H. J. Queisser, J. Appl. Phys. **32**(3), 510–519 (1961).

[31]T. Tiedje, E. Yablonovitch, G. D. Cody, and B. G. Brooks, IEEE Trans. Electron Devices **31**(5), 711–716 (1984).

[32]M. A. Green, IEEE Trans. Electron Devices **31**(5), 671–678 (1984).

[33]J. H. Werner, S. Kolodinski, and H. J. Queisser, Phys. Rev. Lett. **72**(24), 3851–3854 (1994).

[34]M. A. Green, Prog. Photovoltaics **7**, 327–330 (1999).

[35]F. Dross, K. Baert, T. Bearda, J. Deckers, V. Depauw, O. El Daif, I. Gordon, A. Gougam, J. Govaerts, S. Granata, R. Labie, X. Loozen, R. Martini, A. Masolin, B. O'Sullivan, Y. Qiu, J. Vaes, D. Van Gestel, J. Van Hoeymissen, A. Vanleenhove, K. Van Nieuwenhuysen, S. Venkatachalam, M. Meuris, and J. Poortmans, Prog. Photovoltaics **20**(6), 770–784 (2012).

[36]J. Dore, D. Ong, S. Varlamov, R. Egan, and M. A. Green, IEEE J. Photovolt. **4**(1), 33–39 (2014).

[37]V. Depauw, Y. Qiu, K. Van Nieuwenhuysen, I. Gordon, and J. Poortmans, Prog. Photovoltaics **19**(7), 844–850 (2011).

[38]E. Yablonovitch, J. Opt. Soc. Am. A **72**(7), 899–907 (1982).

[39]M. A. Green, Prog. Photovoltaics **10**, 235–241 (2002).

[40]S. Mokkapati and K. R. Catchpole, J. Appl. Phys. **112**, 101101 (2012).

[41]C. Battaglia, M. Boccard, F. J. Haug, and C. Ballif, J. Appl. Phys. **112**, 094504 (2012).

[42]J. Oh, H. C. Yuan, and H. M. Branz, Nat. Nanotechnol. **7**, 743–748 (2012).

[43]A. Mavrokefalos, S. E. Han, S. Yerci, M. S. Branham, and G. Chen, Nano Lett. **12**, 2792–2796 (2012).

[44]E. D. Palik, Handbook of Optical Constants of Solids (Academic, Orlando, 1985).

[45]D. K. Schroder, IEEE Trans. Electron Devices **44**(1), 160–170 (1997).

[46]O. Deparis, Opt. Lett. **36**(20), 3960–3962 (2011).

[47]M. Liscidini, D. Gerace, L. C. Andreani, and J. E. Sipe, Phys. Rev. B **77**(3), 035324 (2008).

[48]R. Brendel, M. Hirsch, R. Plieninger, and J. H. Werner, IEEE Trans. Electron Devices **43**(7), 1104–1112 (1996).

[49]W. J. Yang, Z. Q. Ma, X. Tang, C. B. Feng, W. G. Zhao, and P. P. Shi, Sol. Energy **82**, 106–110 (2008).

[50]K. L. Luke and L. Cheng, J. Appl. Phys. **61**(6), 2282–2293 (1987).

[51]R. K. Ahrenkiel and S. W. Johnston, Sol. Energy Mater. Sol. Cells **93**, 645–649 (2009).

[52]*Thin Film Solar Cells*, edited by J. Poortmans and V. Arkhipov (John Wiley & Sons Ltd., Chichester, 2006), Chap. 4.

[53]*Thin–Film Silicon Solar Cells*, edited by A. Shah (EPFL Press, Lausanne, 2010), Chap. 3.

[54]A. G. Aberle, Prog. Photovoltaics **8**, 473–487 (2000).

[55]E. Yablonovitch, D. L. Allara, C. C. Chang, T. Gmitter, and T. B. Bright, Phys. Rev. Lett. **57**(2), 249–252 (1986).

[56]M. Otto, M. Kroll, T. Käsebier, R. Salzer, A. Tünnermann *et al.*, Appl. Phys. Lett. **100**, 191603 (2012).

[57]M. Berginski, J. Hüpkes, A. Gordijn, W. Reetz, T. Wätjen, B. Rech, and M. Wuttig, Sol. Energy Mater. Sol. Cells **92**(9), 1037–1042 (2008).

[58]V. Jovanov, U. Planchoke, P. Magnus, H. Stiebig, and D. Knipp, Sol. Energy Mater. Sol. Cells **110**, 49–57 (2013).

[59]V. Depauw, X. Meng, O. El Daif, G. Gomard, L. Lalouat, E. Drouard, C. Trompoukis, A. Fave, C. Seassal, and I. Gordon, IEEE J. Photovolt. **4**(1), 215–223 (2014) .